First-principles local-orbital density-functional study of Al clusters

Sang H. Yang
Physics Department, University of Illinois, Urbana, Illinois 61801

David A. Drabold
Department of Physics and Department of Materials Science and Engineering, University of Illinois, Urbana, Illinois 61801

James B. Adams
Department of Materials Science and Engineering, University of Illinois, Urbana, Illinois 61801

Amit Sachdev
Department of Chemical Engineering, University of Illinois, Urbana, Illinois 61801
(Received 26 February 1992; revised manuscript received 8 September 1992)

We report *ab initio* molecular-dynamics simulations of small aluminum clusters, Al_n of $n=2-6$ and 12, 13, 55, and 147, using the density-functional, local-orbital method of Sankey. Equilibrium structures and total energies were calculated and compared with experiment and the predictions of other calculations. The minimum energy structure of Al_{13} and Al_{55} are found to be distorted icosahedrons, whereas that of Al_{147} appears to be a slightly distorted cubo-octahedron. The vibrational density of states was calculated for most of these clusters. We also performed embedded-atom method calculations for Al_{13}, Al_{55}, and Al_{147} and compared these calculations to the *ab initio* calculations.

I. INTRODUCTION

Metal clusters have been studied extensively during the last decade.[1-7] The structure and properties of clusters can be dramatically different from the bulk due to the high surface area to volume ratio.[7] The addition of a few atoms can result in major structural rearrangements.[8]

Some of the major questions in the study of clusters are: what kind of structure do clusters have at their energy minima; at what size does a cluster exhibit a bulklike structure;[9] how does the insulator-metallic transition occur in a metal cluster as the cluster size increases?[8] All these questions depend strongly on cluster size and geometry.

In general, clusters of noble gases are expected to be icosahedral structures (ICS's) because of their weak and isotropic interatomic interactions. Therefore, their atomic packing behaves like billiard balls.[8] In a billiard-ball model, an ICS has a more compact form than a cubo-octahedral structure (COS), for the ICS has a higher coordination number than the COS for a given cluster size.[7] Note that the COS is face-centered-cubic. In metal clusters, however, the problem becomes more complicated because of the existence of the angular force derived from occupied p or d orbitals.

On the experimental side, an electron-diffraction study on argon clusters showed that an argon cluster is icosahedral up to $n=1500$ atoms.[10,11] Another study on Pd clusters conducted with scanning transmission electron diffraction (STED) showed that Pd clusters with diameters less than 20 Å also prefer the non-fcc icosahedral over the standard fcc structure on substrates of TiO_2 and Al_2O_3.[12] On the other hand, a study of Cu clusters on a carbon substrate with extended x-ray-absorption fine structure (EXAFS) indicated that a Cu cluster has a fcc structure even at about thirteen atoms.[13] Another metal cluster study of Au clusters on SiO_2 indicated that the fcc structure seems to be favored over ICS for a diameter bigger than 20 Å.[14] Other transition metals (Pt, Rh, Ni, and Ag) are believed to behave similarly to Au.[14,15]

On the theoretical side, classical potentials were used in studying the minimum-energy structures of noble gases. The ICS's were found to be more stable than the COS's for clusters having less than a few thousand atoms.[16,17] One classical empirical potential, embedded-atom method (EAM), has been very good in predicting the bulk and surface structure of certain metals.[18] Some calculations have been performed on clusters.[19-22] Sachdev and Masel have done an extensive study on Pt from 5- to 60-, and 147-atom clusters with EAM.[22] They found that the equilibrium structures of all of those clusters were greatly distorted from ideal ICS's or COS's, including the magic number clusters of 13 and 55 atoms.

Jellium models have been adopted to investigate the properties of metal clusters.[8] This model assumes that both positive background and negative electron charges are distributed uniformly over a sphere. Milani, however, indicates that in aluminum the assumption of jellium yields incorrect polarizations and ionization potentials if the cluster is less than $n=40$.[23]

Upton used a jellium scheme on his calculations of small aluminum clusters. The exact electron-nuclear attraction potential was used as a perturbation on the smooth spherically symmetric potential of the jellium model (droplet model).[24] Cheng and Berry used density-functional theory (DFT) within the discrete-variational-method X_α scheme, and found the electronic structures and binding energies of aluminum 13-, and 43-, and 55-

atom clusters with perfect icosahedral and cubo-octahedral symmetry.[15] Yi *et al.* used the Carr-Parrinello scheme to study the ideal ICS and COS for 13-, 19-, and 55-atom aluminum clusters[7] and to find minimum-energy structures of 13- and 55-atom aluminum clusters.[25] A better calculation has been done on small aluminum clusters of less than ten atoms by Jones, who used the local-spin-density (LSD) approximation within DFT.[1] Table I summarizes their results on aluminum clusters.

To study the energy and structure of aluminum clusters, we use Sankey's scheme,[26] which involves the local-density approximation (LDA) within DFT. Unlike other LDA calculations implemented in reciprocal space with a plane-wave basis set, this method uses local orbitals in *real space.* Applications of this method to Si (Ref. 27) and C (Ref. 28) in a variety of bonding environments yielded results very close to state of the art electronic structure calculations.

We briefly discuss the theoretical background of this method in Sec. II, and outline the computational procedures in Sec. III. The results are given in Sec. IV, of which the first part deals with the energy, structure, and vibrational spectra of small aluminum clusters of two to six atoms. The second part of the results section discusses the energy, structure, and vibrational spectra of the medium-sized clusters (12–147). As the last part of this section, EAM calculations are carried out on these medium-sized clusters. The conclusion appears in the final section.

II. GENERAL THEORY AND METHOD

The theoretical foundation of this method is the LDA within DFT.[26] LDA estimates the density-functional exchange-correlation term from calculations on the homogeneous electron gas. We use the Ceperley-Alder potential[29] as parameterized by Perdew and Zunger.[30] Based on this foundation we use three more approximations, which have been tested thoroughly.

First, we use a non-self-consistent version of the DFT by using a linearized form of the Kohn-Sham equations due to Harris and Foulkes.[31,32] The advantage of this approximation over the conventional Kohn-Sham method is that we only need to solve the electronic eigenvalue problem once for each atomic configuration instead of about ten times for typical self-consistent methods. Another advantage of this approximation is that it avoids evaluating four center Coulomb integrals.[26] The justification of this Harris functional was provided by Harris,[31] Polatoglou and Methfessel,[33] and Read and Needs[34] on various types of materials such as metals, semiconductors, and NaCl, a highly ionic compound. They found excellent agreement with the fully self-consistent calculations.

Second, we approximate the one-electron-energy eigenstate as linear combination of pseudoatomic orbitals (PAO),[35] computed from a self-consistent Herman-Skillman-like program.[36] We impose a confinement boundary R_c to reduce the number of neighbors interacting with a site. Beyond R_c there is no interaction.

TABLE I. Aluminum clusters calculation.

Size	Upton (Ref. 24)	Jones (Ref. 1)	Cheng and Perry (Ref. 15)	Yi *et al.* (Refs. 7 and 25)	This work
2		linear (2.71 Å)[a] (2.48 Å)[b]			linear (2.95 Å)[a] (2.47 Å)[b]
3	isos. tri. (2.62 Å) (2.63 Å)	equ. tri. (2.46 Å)			equ. tri. (2.52 Å)
4	rhombus (2.61 Å) ($\alpha=70.2°$)	rhombus (2.52 Å) ($\alpha=56.5°$)			nearly rhombus (2.54, 2.53 Å) ($\alpha=64.5°$)
5	squ. pyramid (C_{2v})	pyramid (C_s)			planar (C_{2v})
6	bipyramid. (D_2)	dist. bipy. (D_{3d})			dist. bipy. (D_{3d})
13				s. dist. ICS[c]	s. dist. ICS[c]
55				dist. ICS[d]	dist. ICS[d]
147					s. dist. COS
ideal[e] 13			ICS	ICS	ICS
ideal[e] 19				COS	
ideal[e] 55			COS	COS	COS
ideal[e] 147					COS

[a]The lowest-energy structure of Al_2. The corresponding experimental value is 2.70 Å (Ref. 40).
[b]The other metastable structure of Al_2. The corresponding experimental value is 2.47 Å (Ref. 41).
[c]Slightly distorted icosahedral structure.
[d]Significantly distorted icosahedral structure.
[e]Perfect ICS and COS clusters relaxed without symmetry breaking.

The physical interpretation of this boundary is that PAO is slightly excited. An additional rationale for compact orbitals (e.g., without exponential tails) has recently been given by Robertson, Payne, and Heine, using self-consistent plane-wave methods.[37] For Al they observe a contraction of the spherical fragment charge density relative to the free-space PAO. Our confinement boundary condition mimics this effect.

Finally, we use the nonlocal, norm-conserving pseudopotentials of the Bachelet, Hamann, and Schluter type,[38] which are angular-momentum dependent. These nonlocal pseudopotential matrix elements are calculated exactly in our method.

III. SIMULATION

To find the equilibrium structures of aluminum clusters, we employ both the dynamic quenching[26] and steepest descent techniques. The force acting on an atom at a position in space is determined by taking the derivative of the total energy with respect to the position vector.

To study a large volume of the cluster configuration space, we employ an adaptation of a method first used on amorphous Si.[39] In this scheme, we start with ideal structures (the ICS and the COS) and introduce disorder by giving the cluster large kinetic temperatures of 500–8000 K, and allow the system to evolve for a time long enough that the cluster becomes highly disordered. We then seek energy minima from a variety of evolution times. In this fashion we can generate a large collection of energy minima and thus be more likely to discern the ground-state structures of the cluster.

The vibrational power spectrum[26] was calculated for the small clusters. It is the Fourier cosine transformation of the velocity-velocity autocorrelation function.[26] For these calculations the initial conditions of atoms in a cluster were constrained in such a way that the center of mass is fixed at one point in space and the cluster has zero angular momentum.

IV. RESULTS

A. Small Clusters

The geometry of Al_n, $n=2-6$, is shown in Fig. 1 with the binding energies per atom in eV. The third column lists the structures with the lowest energies.

Dynamic quenching of Al_2 gives two different minimum-energy states, of which the ground state of the dimer has a bond length of 2.95 Å. The corresponding experimental value was 2.70 Å,[40] which was estimated from vibrational spectra of aluminum dimers. Such a discrepancy is to be expected for a spin-unpolarized (LDA) calculation. For larger systems this does not pose a significant problem. The single harmonic-vibrational mode is calculated to be $\omega=246$ cm^{-1} (see Fig. 2), in reasonable agreement with the experimental value of 284.2 cm^{-1}.[40] The other metastable state of the aluminum dimer has a bond length of 2.47 Å and the single harmonic-vibrational frequency of 372 cm^{-1}, close to the

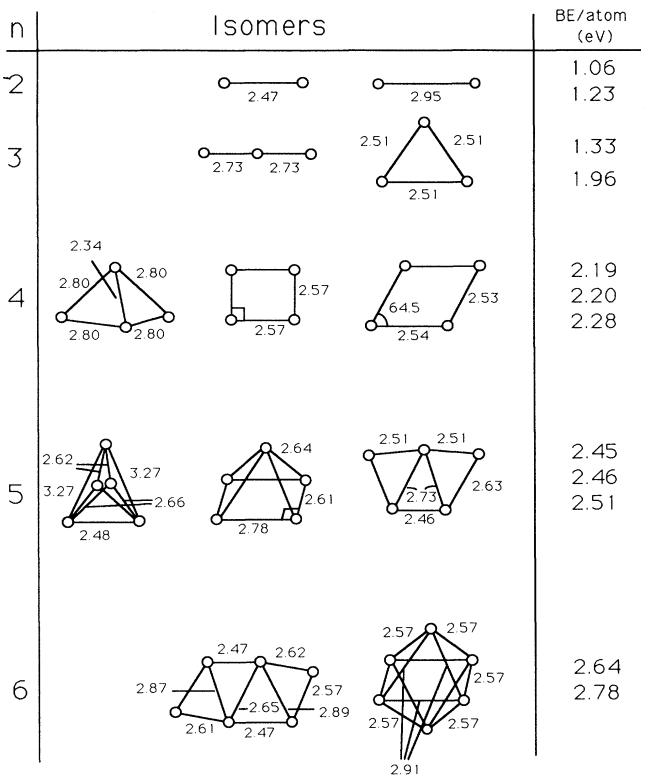

FIG. 1. Minimum-energy structures of Al_n, $n=2-6$ with the binding energies per atom. Third column's structures are believed to be the minimal energy structures.

experimental results of 2.47 Å and 350.01 cm^{-1}, respectively.[41,42]

The existence of two different minimum-energy states for Al_2 becomes clear when we consider the total energy of Al_2 as a function of the distance between atoms, plotted in Fig. 3. There is a discontinuity in the slope, and two different local minima. Figure 4 shows the eigenvalues of the one-electron LDA Hamiltonian for Al_2 with respect to the separation distance. There are six valence electrons in Al_2, and the two lowest molecular levels, $1\sigma_g$

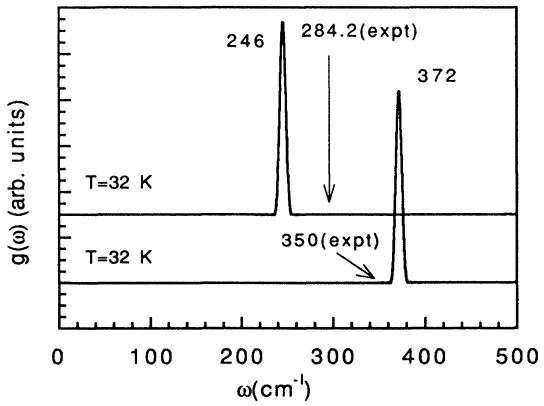

FIG. 2. Vibrational power spectra of Al_2 in the two lowest-energy structures at a temperature of 32 K.

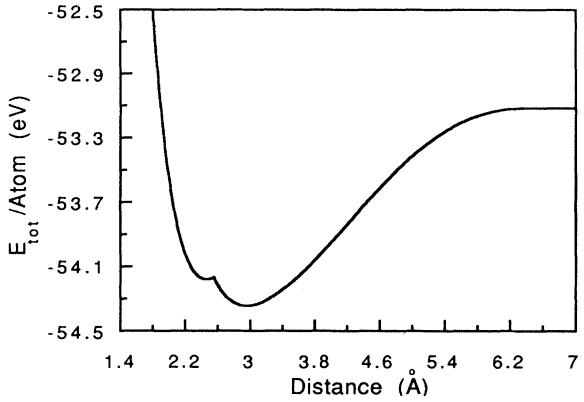

FIG. 3. Total energy per atom Al_2 as a function of an aluminum dimer bond length. There are two energy minima.

and $1\sigma_u$ are filled by four spin-degenerate electrons. At $d=2.95$ Å, the molecular level $2\sigma_g$ is fully filled by the other two electrons; however, as the Al-Al distance decreases the $2\sigma_g$ level crosses the fourfold-degenerated level $1\pi_u$ at 2.55 Å, resulting in a new equilibrium state at a smaller separation of 2.45 Å. This is why there are two minima on the potential-energy surface of an aluminum dimer.

The ground state of Al_3 is found to be an equilateral triangle with a bond length of 2.51 Å (see Fig. 1). This is in good agreement with the more rigorous LSD approximation of Jones, who also finds an equilateral triangle with $d=2.46$ Å.[1] Upton finds the same structure with $d=2.62$ Å.[24] Figure 5 shows the one-electron Hamiltonian eigenvalues as a function of θ, the angle of an isosceles triangle with the side length d kept at its equilibrium value of 2.51 Å. There are nine valence electrons in Al_3. The molecular-energy levels from the first to the fourth are filled completely by eight electrons. The fifth level is the highest occupied level (Fermi level), which is partially filled with one electron (see Fig. 5).

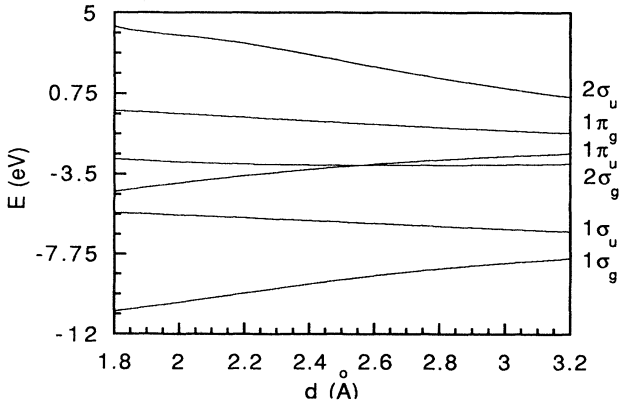

FIG. 4. Eigenvalues of the one-electron LDA Hamiltonian for Al_2 as a function of an aluminum dimer bond length. The level crossing corresponds to existence of two different minimum-energy states.

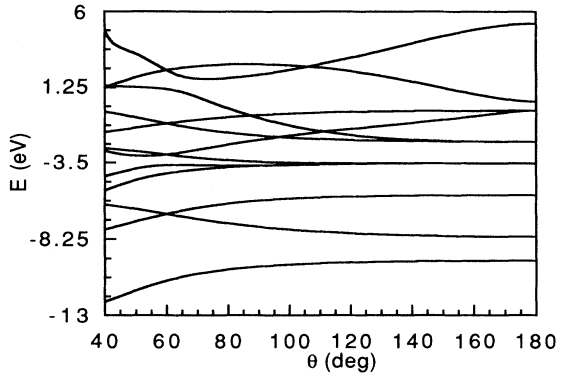

FIG. 5. The one-electron LDA energy eigenvalues as a function of the open angle θ of an isosceles triangle, Al_3, with the fixed-side length of its equilibrium value, 2.51 Å. The absence of a degenerate state at the Fermi level suggests the minimum-energy structure; the equilateral triangle is electronically stable.

The total energy as a function of θ with fixed d is shown in Fig. 6. It clearly shows $\theta=60°$ is the ground-state structure. By symmetry, the structure with $\theta=300°$ is another minimum. There is a relatively large potential barrier that the molecule Al_3 needs to overcome as it passes through $\theta=180°$. There exists shallow local energy minimum at $\theta=180°$, as in the case of Si_3.[27] Indeed, a linear molecular structure was found to be a metastable structure. The optimal bond length is 0.22 Å longer, and the energy is 0.63 eV/atom higher than the equilateral triangle. The vibrational frequency modes are calculated for the equilateral triangle shown in Fig. 7. The peaks correspond to the $3n$-6 normal modes of vibration.

The several local minimum structures found for Al_4 are shown in Fig. 1. The most stable form of Al_4 is a parallelogram with side lengths of 2.54 and 2.53 Å (very similar to a rhombus) and a bond angle of 64.5°, which compares well with Jones' result of a rhombus with a side length of 2.52 Å and an angle of 56.5° shown in Table I.[1] Note that Upton's less exact method disagrees with these planar-type structures. His minimum-energy structure

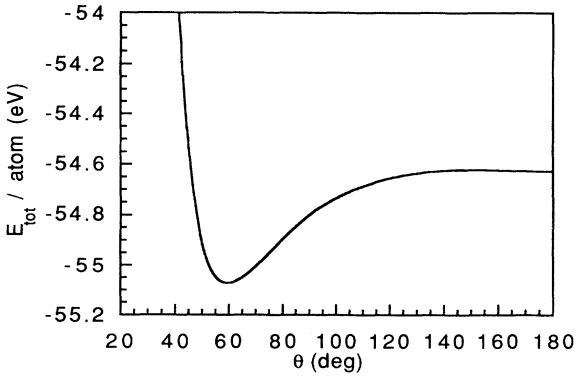

FIG. 6. The total energy per atom of Al_3 as a function of the opening angle of an isosceles triangle with the fixed-side length of its equilibrium value, 2.51 Å.

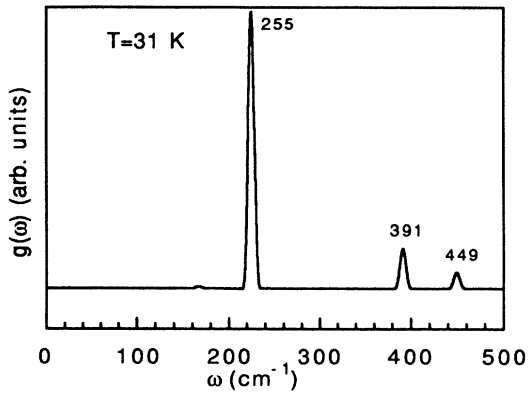

FIG. 7. The vibrational spectral density $g(\omega)$ of Al_3 in its lowest-energy structure at the low kinetic temperature of 31 K.

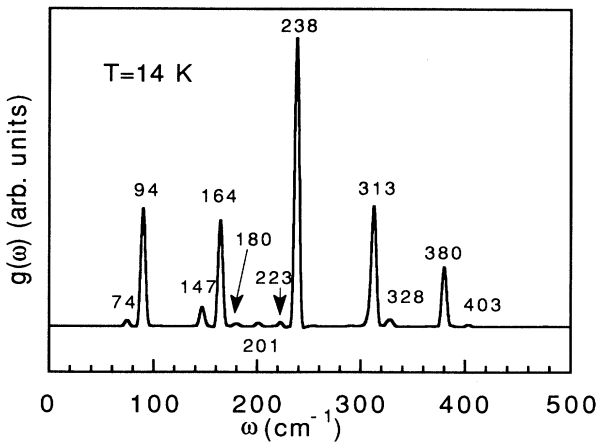

FIG. 8. Vibrational spectral density $g(\omega)$ of Al_6 in its lowest-energy structure at the low kinetic temperature of 14 K.

for Al_4 is three dimensional with C_{2v} symmetry. The other local minimum-energy structures include a square and tetrahedron with the side lengths of 2.57 and 2.80 Å, respectively (see Fig. 1).

The minimum-energy structure of Al_5 is found to be a planar C_{2v} structure. It is W shaped with the side length 2.63 Å, shown in Fig. 1. Pyramid and trigonal bipyramid structures are metastable structures. They are almost degenerate with an energy difference less than 0.01 eV/atom. The total energy of either structure is about 0.05 eV/atom higher than that of the planer C_{2v} form. In contrast to our results, Jones and Upton find that a pyramid is the minimum-energy configuration for Al_5 (see Table I).[24]

The minimum-energy structure of Al_6 is a distorted bipyramid with bond lengths of 2.57 and 2.91 Å, with D_{3d} point-group symmetry, shown in Fig. 1. This agrees well with Jones' result of a D_{3d} structure with bond lengths of 2.52 and 2.87 Å. Upton finds his minimum-energy structure to be a square-based bipyramid of the D_2 point-group symmetry. We find that the other metastable structure for Al_6 to be a planar shape with C_{2v} symmetry. It is 0.14 eV/atom higher in energy than the minimum-energy structure. The vibrational frequency of the minimum-energy structure of Al_6 is shown in Fig. 8. Twelve modes can be distinguished at the temperature of 14 K.

Note that a structural transition from the planar to the three-dimensional occurs at $n=6$. In Jones' case it occurs at $n=5$, while in Upton's case it happens at $n=4$. We are not aware of a simple explanation for this discrepancy.

B. Medium clusters

The medium-sized cluster of 12 atoms, and the magic number clusters of 13, 55, and 147 atoms are considered in this study. The cluster symmetries examined are the ICS and the COS, since they are expected to be the most stable. The COS (or fcc) are characterized by the presence of square (100) and triangular (111) facets on their surface, while the ICS's are characterized by only (111) facets (see Fig. 9).[22] The closed-shell numbers (magic number) of both of these structures are 13, 55, and 147 for the first, second, and third shells, respectively. As an example, in a 13-atom cluster, there are 12 atoms surrounding a central atom in the first shell. For clusters made of rare gases, which exhibit short-range and isotropic potentials, ICS's are expected to be more stable than the COS, because the ICS's have greater average coordination numbers (6.5 and 8.5 versus 5.5 and 7.9 for the 13-

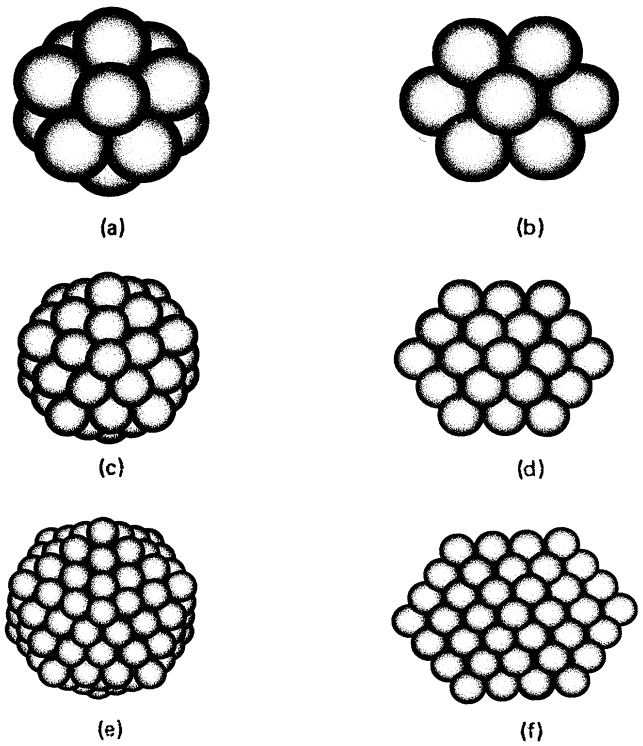

FIG. 9. Shapes of ideal ICS and COS of the magic numbers 13, 55, and 147. (a), (c), and (e) are ICS of 13, 55, and 147 atoms. (b), (d), and (f) are COS of 13, 55, and 147 atoms. The minimum-energy structure of Al_{13} is almost the same as (a).

and 55-atom clusters of the ICS and the COS, respectively).[25] In aluminum, however, there is the angular force created from valence p orbitals. The effects of this force might be substantial.

We investigate the property of these magic number clusters by seeking minimum-energy structures through Sankey's method. At the end of this section we will also present the investigation of these clusters with the EAM. Table I summarizes our results.

First, we compare the energy of the ideal ICS and COS of aluminum clusters relaxed without symmetry breaking. For a 13-atom cluster this ICS is lower in energy than the COS by 0.14 eV/atom, while the reverse is true for the 55 and 147 by 0.03 and 0.02 eV/atom, respectively. These results are in good agreement with the calculations carried out by Yi *et al.*, Cheng and Berry.[7,15] Yi *et al.* find that the ICS is 0.05 eV/atom lower in energy than the COS for Al_{13}, while the opposite is true for Al_{55} by about 0.04 eV/atom. Cheng and Berry also found the same pattern with the values of about 0.1 and 0.01 eV/atom, respectively. For these ideally relaxed structures, the structural transition from ICS to COS occurs at the cluster size somewhere between 13 and 55 atoms.

However, all of these ideal structures are electronically unstable. The minimum-energy structures are expected to be at least somewhat distorted from their ideal structures partly due to the Jahn-Teller effect. For example, in the ideal ICS of Al_{13}, the highest occupied one-electron-energy eigenvalue is triply degenerate (or sixfold degenerate including spin) with five electrons occupied on the level, which makes the cluster Jahn-Teller unstable. In addition to the distortion from this electronic instability, the high ratio of surface atoms to interior atoms in clusters is likely to cause geometric distortions.

The minimum-energy structure of Al_{13} turns out to be a very slightly distorted ICS. Many of the above quenching runs result in this structure. For example, both the direct dynamic quenching of an ideal ICS and another dynamic quenching of an ideal COS initially heated to 8000 K for 125 fs lead to the same structure. Its total energy is very close (less than 0.01 eV/atom) to that of the ideal ICS relaxed without symmetry breaking. The distortion of this structure from the ideal ICS is so small that we are able to find its distortion only by comparing the distances measured from a central atom to each surrounding atom, and comparing the electronic states of two structures near their Fermi levels, not by looking at three-dimensional pictures. Clearly the Jahn-Teller distortion is extremely small for this cluster.

For this minimum-energy structure of Al_{13}, the distances from a central atom to its neighbors are either 2.63 or 2.53 Å, while for the ideal ICS all the distances are consistently 2.60 Å. This is a fairly small departure from perfect icosahedral symmetry. The symmetry breaking occurs naturally in the molecular-dynamics (MD) simulation from the triply degenerate level (excluding spin) of the ideal ICS into two different levels, leaving no degeneracy at the highest occupied level of the minimum-energy structure. Yi *et al.* also find that a slightly distorted (ICS) is electronically more favorable than an ideal ICS by 0.02 eV/atom.[25] The vibrational spectrum is shown in Fig. 10. It becomes complex due to the size of the cluster.

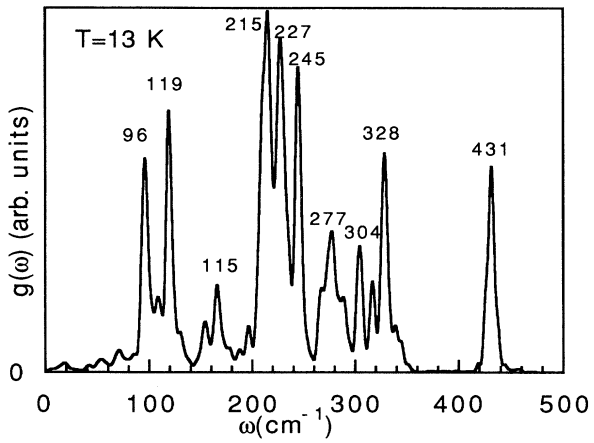

FIG. 10. Vibrational spectral density $g(\omega)$ of Al_{13} in its lowest-energy configuration at the low kinetic temperature of 13 K.

To increase our understanding of Al_{13}, similar methods were used to find the optimal structure of Al_{12}. The starting configurations were an ideal ICS and COS of Al_{13} with a missing atom. These ideal structures were quenched after heating at various temperatures. The minimum structure of Al_{12} is found to be very distorted from the ideal structures. But it is certain that it has an icosahedral origin (see Fig. 11). The binding energy per atom is 3.38 eV.

Annealing of the ideal ICS and COS of Al_{55} resulted in an unusual structure (see Fig. 12). This structure appears to be a distorted ICS. This is unexpected, since the ideal COS is energetically more favorable than the ideal ICS. This structure was found by quenching an ideal ICS initially heated to 500 K for 375 fs. This structure is lower in energy than the ideal COS relaxed without symmetry breaking by 0.05 eV/atom. This compares well with the results presented by Yi *et al.*, who also find the minimum-energy structure to be a very distorted ICS, which is lower in energy than the ideal COS by 0.1 eV/atom.[25] We also found that there are many other similar structures with nearly the same energy with the lowest-energy structure. The energy differences with all those are less than 0.02 eV/atom.

The minimum-energy structure of Al_{147} is found to be

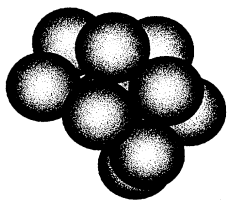

FIG. 11. The minimum-energy structure of Al_{12}. It is a distorted ICS.

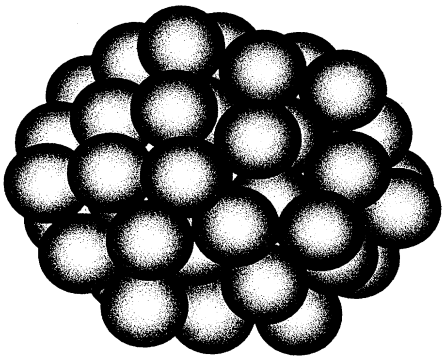

FIG. 12. The lowest-energy configuration of Al_{55}. It is a distorted ICS.

a slightly distorted COS, shown in Fig. 13. It looks as if the edges of the square are either squeezed or pulled out slightly. This structure was obtained by a direct dynamic quenching of the ideally relaxed COS without heating it at all. The distortion from the ideal COS is due to the Jahn-Teller effect. In the ideal COS, the highest occupied molecular level is triply degenerate (excluding spin). During molecular-dynamic simulations this level splits into three different levels, resulting in no degeneracy at the highest occupied level of the minimum-energy structure. Many other different structures were obtained by employing dynamic quenchings of the ideal ICS and COS, initially heated to 8000 K for various times of 24–1000 fs. All of these structures have their energies at least 0.01 eV/atom larger than the minimum-energy

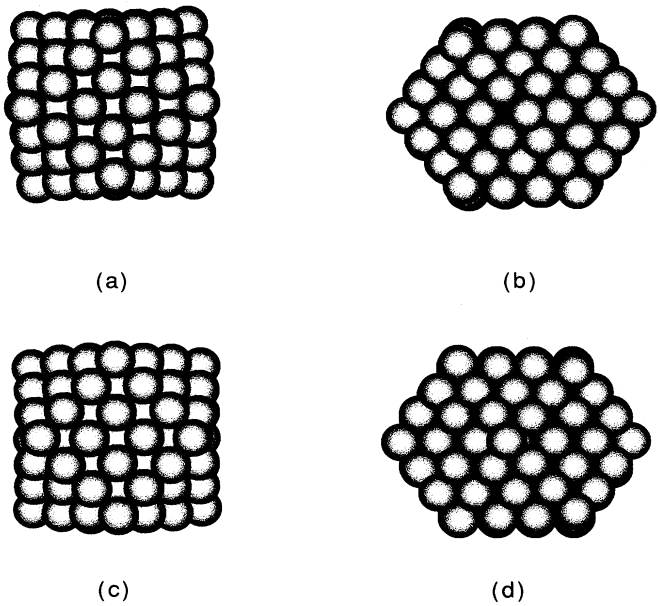

FIG. 13. The minimum-energy structure of Al_{147}. It is slightly distorted from an ideal COS. It is viewed from four different perspectives. (a) is the front view. (b) is 45° rotated from (a). (c) is 90° rotated from (a). (d) is 135° rotated from (a).

COS, except a nearly perfect ICS, which is obtained from a direct dynamic quenching of the ideal ICS or another quenching of the same ideal structure initially heated to 8000 K for 311 fs. This ICS is nearly degenerate with the minimum-energy COS. The energy difference between these two structures is about 0.0016 eV/atom.

One of the main questions in the study of metal clusters is at which size does the structural transformation from ICS to COS (bulklike) occur. The bulk structure of aluminum is known to be the COS (fcc). For Al_{13} and Al_{55} the lowest-energy structures are the distorted ICS. The Al_{13} is the almost perfect ICS, and the Al_{55} is the very distorted ICS. However, for Al_{147} the minimum-energy structure is found to be the almost perfect COS, whose energy is about 0.002 eV/atom lower than that of the next-lowest-energy structure, the nearly perfect ICS. This implies that the structural transformation from ICS to COS (bulklike) occurs very near 147 atoms, as shown in Fig. 14.

The binding energy per atom is shown in Fig. 15 for the most stable structures. It rapidly approaches a calculated bulk value of 4.36 eV/atom. The experimental value is 3.39 eV/atom.[43] The lattice constant of bulk aluminum is calculated to be 3.94 Å, which is somewhat smaller than the experimental value of 4.03 Å.[43] The errors of the binding energy and lattice constant are from an incomplete basis set of local orbitals. We only include s and p orbitals as the basis set. Jansen and Klein show that adding d orbitals in the basis set yields an essentially exact LDA band structure for crystalline Al.[44] In addition to the basis-related effects, there is a well-known tendency of LDA to overbind.

One of the other major questions of metal clusters is how the insulator-metallic transitions occurs as the cluster size increases. One way to answer this might be by

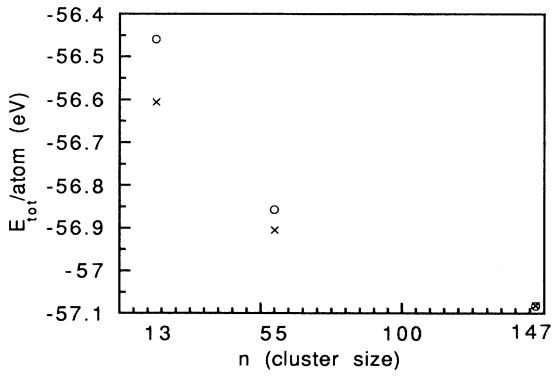

FIG. 14. Comparison of energetics of ICS and COS clusters. o (x) denotes COS (ICS) symmetric clusters. o's of 13 and 55 atoms are the ideal COS's relaxed without symmetry breaking. o of 147 atoms is the minimum-energy structure in its size, which is an almost perfect COS. x's of 13 and 55 atoms are the minimum-energy structures in their sizes, almost perfect ICS's and very distorted ICS's, respectively. x of 147 atoms is the lowest-energy configuration in icosahedral form, which is 0.0016 eV/atom higher in energy than o of 147 atoms. The structural transformation from ICS to COS (bulklike) appears to occur around $n = 147$.

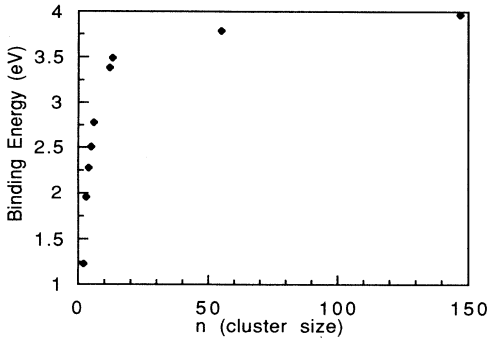

FIG. 15. Binding energies of the minimum-energy structures vs cluster size n.

calculating the ionization potentials of clusters. The clusters are easily classified as metallic, nonmetallic, or semiconducting in terms of their ionization potential. The other way to answer this question is by measuring the band-structure energy gap. However, the lack of translational periodicity in clusters excludes this possibility. We instead consider HOMO-LUMO gaps of Al clusters. That is the gap between the highest occupied molecular orbital and the lowest unoccupied molecular orbital energy (HOMO-LUMO) of a cluster.

Figure 16 shows HOMO-LUMO gaps plotted against cluster size. All those gaps are measured from the minimum-energy structure except $n=54$ and 146. The plot certainly shows that aluminum becomes more metallic as the size of a cluster increases in large clusters, approaching 0, the bulk value. The HOMO-LUMO gaps at $n=55$ and 147 are close to 0, the bulk value. On the other hand, the plot shows that the gap increases in small

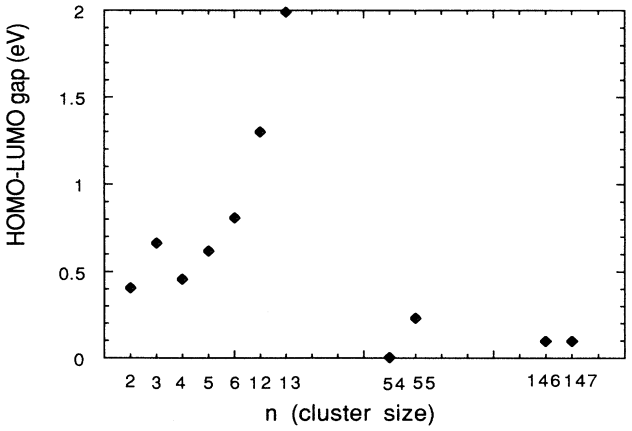

FIG. 16. The HOMO-LUMO gap. All these gaps are calculated for the minimum-energy structures vs cluster size except $n=54$ and 146 atoms. These two structures were obtained from direct dynamic quenchings of ideal structures and ICS's and COS's with a missing atom, respectively. The $n=54$ is a highly distorted ICS and the $n=146$ is almost indistinguishable from an ideal COS with one vacancy. The metallicity increases as the cluster size increases, decreases as the degree of geometrical symmetry in a cluster increases.

size clusters as the cluster size increases from 2 to 13 atoms. Our results may be compared with the experimental results of ionization potential. An experimental trend for the ionization potential of Al clusters is that it grows steadily to a maximum value at Al_6,[45] and there is a drop at Al_7.[5] Note that in Fig. 16 the HOMO-LUMO gaps are relatively high at $n=3$, 6, and 13. All these numbers correspond to highly symmetric structures in our case. $n=3$ is an equilateral triangle, and $n=6$ is a D_{3d} structure, and $n=13$ is the almost ideal ICS. To support this idea we obtain two more structures for $n=54$ and 146. Those two are not minimum-energy structures. The structures were obtained by employing direct dynamic quenchings to an ideal ICS of 55-atom and COS of 147-atom clusters with a missing atom in each case. For the 54-atom cluster, the quenching yielded a quite distorted ICS, while for the 146-atom cluster it yielded an almost indistinguishable structure from the ideal COS with one vacancy. The 146-atom cluster preserves its symmetry well, while the 54-atom cluster does not. Figure 16 shows that the HOMO-LUMO gap for the 54-atom cluster is much smaller than the 55-atom (magic number) cluster, while that of the 146-atom cluster almost same as the 147-atom (magic number) one. Our results empirically suggest that Al clusters become more metallic as the size increases and less metallic as the degree of geometrical symmetry in structures increases. The first one dominates for larger clusters, while the latter one dominates for small-sized clusters.

An EAM calculation has been performed using Voter's potential for Al clusters.[46] The results are presented in Table I along with the calculations using Sankey's method. In the ideal structures relaxed without symmetry breaking, the EAM calculations reveal that the ideal ICS's are lower in energy than the ideal COS's for all Al_{13}, Al_{55}, and Al_{147} clusters, while in the Sankey's method, these are only true for 13-atom clusters, not for 55- and 147-atom clusters. In fact, for the EAM, the minimum-energy structures of all magic number clusters of Al_{13}, Al_{55}, and Al_{147} are these ideal ICS's . In Sankey's method the minimum-energy structures for Al_{13} and Al_{55} are the ICS's, while that of Al_{147} is the slightly distorted COS, which is nearly degenerate with the slightly distorted ICS. Thus, the EAM results are qualitatively reasonable in a sense that they predict the ICS for the minimum-energy structures of Al_{13} and Al_{55} and show a correct trend in that the energy difference between the minimum-energy structures and the ideal COS decreases as cluster size increases, as shown in Table II. However, they do not correctly predict the distortions present in those clusters.

V. CONCLUSIONS

Ab inito molecular-dynamics simulations of small aluminum clusters, Al_n of $n=2-6$ and 12, 13, 55, and 147 have been performed with the density-functional, local orbital method of Sankey. EAM calculations have been carried out for Al_{13}, Al_{55}, and Al_{147}.

(1) For Al_2 there are two different local minimum states in agreement with experiment. The minimal ener-

TABLE II. The binding energy (BE) per atom calculated by both density-functional and EAM methods for 13-, 55-, and 147-atom clusters. The ideal ICS and COS relaxed without symmetry breaking and the minimum-energy structures are found by both density-functional and EAM methods.

	BE/atom (tot. BE) eV Density functional	BE/atom (tot. BE) eV EAM
13 atoms		
ideal COS	3.34 (43.44)	2.39 (31.10)
ideal ICS	3.48 (45.30)	2.46 (31.98)
min.	3.49 (45.33)	2.46 (31.98)
min. stru.	sligh. dist. ICS	ideal ICS
55 atoms		
ideal COS	3.74 (205.7)	2.81 (154.6)
ideal ICS	3.71 (204.5)	2.83 (155.7)
min.	3.79 (208.3)	2.83 (155.7)
min. stru.	very dist. ICS	ideal ICS
147 atoms		
ideal COS	3.96 (581.8)	2.98 (437.9)
ideal ICS	3.94 (579.4)	2.99 (438.8)
min.	3.97 (583.0)	2.99 (438.8)
min. stru.	sligh. dist. COS	ideal ICS

gy structure of Al_3 is an equilateral triangle. The absence of a degenerate state at the Fermi level of this equilateral triangle structure suggests that this structure is electronically stable. The structural transition of the minimum-energy structures from the planar to the nonplanar takes place at $n=6$ in our case, while it takes place at $n=4$ and 5 in Upton and Jones' cases, respectively.

(2) For Al_{13} there is the single well-defined minimum-energy structure, and it is a sightly distorted ICS. The minimum-energy structure of Al_{55} is a much distorted ICS. These results for Al_{13} and Al_{55} are in agreement with Yi *et al.*'s calculation. The minimum-energy structure of Al_{147} appears to be a slightly distorted COS. The structure transition from the ICS to the bulklike structure seems to occur very near $n=147$. However, for Al_{55} and Al_{147}, the optimal structures are nearly degenerate with the COS and ICS, respectively.

(3) Examination of the HOMO-LUMO gap empirically suggests that Al clusters become more metallic as their size increases and less metallic as the degree of geometrical symmetry in their structure increases. The first factor dominates for large clusters, while the latter factor dominates for small-sized clusters.

(4) EAM calculations for Al_{13}, Al_{55}, and Al_{147} predict the minimum-energy structures to be perfect ICS's.

ACKNOWLEDGMENTS

This work was supported by the National Science Foundation Grant No. DMR-9 158 584. We thank the National Center for Supercomputing Applications (NCSA) for the use of the Cray-Ymp. We would like to acknowledge informative discussions with O. Sankey, P. Fedders, R. Martin, J. Yi, R. Masel, and K. Kwon. We thank J. Bernholc for the Al_{13} and Al_{55} coordinates. Finally, we thank S. Foiles, M. Daw, and M. Baskes for sharing their EAM codes with us.

[1]R. O. Jones, Phys. Rev. Lett. **67**, 224 (1991).
[2]W. D. Knight, K. Clemenger, W. A. de Heer, W. A. Saunders, M. Y. Chou, and M. L. Cohen, Phys. Rev. Lett. **52**, 2141 (1984).
[3]W. A. de Heer, W. D. Knight, M. Y. Chou, and M. L. Cohen, Solid State Phys. **40**, 93 (1987).
[4]M. L. Cohen, M. Y. Chou, W. D. Knight, and W. A. de Heer, J. Chem. Phys. **91**, 3141 (1987).
[5]D. M. Cox, D. J. Trevor, R. L. Whetten, and A. Kaldor, J. Phys. Chem. **92**, 421 (1988).
[6]K. J. Taylor, C. L. Pettiette, M. J. Craycraft, O. Chesnovsky, and R. E. Smalley, Chem. Phys. Lett. **182**, 347 (1988).
[7]Jae-Yel Yi, D. J. Oh, J. Bernholc, and R. Car, Chem. Phys. Lett. **174**, 461 (1990).
[8]M. L. Cohen and W. D. Knight, Phys. Today **43**, 42 (1990).
[9]Panel Report, J. Mater. Res. **4**, 704 (1989).
[10]J. W. Lee and G. D. Stein, J. Phys. Chem. **91**, 2450 (1987).
[11]J. Farges, M. F. de Feraudy, B. Raoult, and G. Torchet, J. Chem. Phys. **78**, 5067 (1983).
[12]H. Poppa, R. D. Moorhead, and M. Avalos-Borja, J. Vac. Sci. Technol. A **7**, 2882 (1989).
[13]P. A. Montano, G. K. Shenoy, E. E. Alp, W. Schulze, and J. Urban, Phys. Rev. Lett. **56**, 1285 (1983).
[14]S. Ijima and T. Ichihashi, Phys. Rev. Lett. **56**, 616 (1986).
[15]H.-P. Cheng and R. S. Berry, Phys. Rev. B **43**, 10 647 (1991).
[16]J. G. Allpress and J. V. Sanders, Aust. J. Phys. **23**, 23 (1970).
[17]B. W. Van de Waal, J. Chem. Phys. **90**, 3407 (1987).
[18]C. L. Liu, J. M. Cohen, J. B. Adams, and A. F. Voter, Surf. Sci. **253**, 334 (1991).
[19]M. D. Daw and M. I. Baskes, Phys. Rev. B **29**, 6443 (1984).
[20]H. Hsieh and R. S. Averback, in *Clusters and Cluster Assembled Materials,* edited by R. S. Averback, J. Bernholc, and O.

L. Nelson, MRS Symposia Proceedings No. 206 (Materials Research Society, Pittsburgh, 1991).
[21]C. L. Cleveland and U. Landman, J. Chem. Phys. **94**, 7376 (1991).
[22]A. Sachdev and R. Masel, J. Catal. **136**, 320 (1992).
[23]W. A. de Heer, P. Milani, and A. Chatelain, Phys. Rev. Lett. **63**, 2834 (1989).
[24]T. H. Upton, J. Chem. Phys. **86**, 7054 (1987); **174**, 461 (1990).
[25]Jae-Yel Yi, D. J. Oh, and J. Bernholc, Phys. Rev. Lett. **67**, 1594 (1991).
[26]O. F. Sankey and D. J. Niklewski, Phys. Rev. B **40**, 3979 (1989).
[27]O. F. Sankey, D. J. Niklewski, D. A. Drabold, and J. D. Dow, Phys. Rev. B **41**, 12 750 (1990).
[28]D. A. Drabold, Ruoping Wang, and Stefan Klemm, Phys. Rev. B **43**, 5132 (1991).
[29]D. M. Ceperley and G. J. Alder, Phys. Rev. Lett. **45**, 566 (1980).
[30]J. Perdew and A. Zunger, Phys. Rev. B **23**, 5048 (1981).
[31]J. Harris, Phys. Rev. B **31**, 1770 (1985).
[32]W. M. C. Foulkes and R. Haydock, Phys. Rev. B **39**, 12 520 (1989).
[33]H. M. Polatoglou and M. Methfessel, Phys. Rev. B **37**, 10 403 (1988).
[34]A. J. Read and R. J. Needs, J. Phys. Condens. Matter **1**, 7565 (1989).
[35]R. W. Jansen and O. F. Sankey, Phys. Rev. B **36**, 6520 (1987).
[36]F. Herman and S. Skillman, *Atomic Structure Calculations* (Prentice-Hall, Englewood Cliffs, NJ, 1963).
[37]I. J. Robertson, M. C. Payne, and Volker Heine, J. Phys. Condens. Matter **3**, 8351 (1991).
[38]G. B. Bachelet, D. R. Hamann, and M. Schluter, Phys. Rev. B **26**, 4199 (1982).
[39]D. A. Drabold, P. A. Fedders, and O. F. Sankey, Phys. Rev. B **42**, 5135 (1990).
[40]M. F. Cai, T. P. Djugan, and V. E. Bondybey, Chem. Rev. Lett. **155**, 430 (1989).
[41]D. S. Ginter, M. L. Ginter, and K. K. Innes, Astrophy. J. **139**, 365 (1964).
[42]K. P. Huber and G. Herzberg, *Molecular Spectra and Molecular Structure. IV. Constants of Diatomic Molecules* (Van Nostrand Reinhold, New York, 1979).
[43]C. Kittel, *Introduction to Solid State Physics,* 6th ed. (Wiley, New York, 1986).
[44]R. W. Jansen and B. M. Klein, in *Atomic Scale Calculations in Materials Science,* edited by J. Tersoff, D. Vanderbilt, and V. Vitek, MRS Symposia Proceedings No. 141 (Materials Research Society, Pittsburgh, 1988), p. 13.
[45]L. Hanley, S. A. Ruatta, and S. L. Anderson, J. Chem. Phys. **87**, 260 (1987).
[46]A. F. Voter and J. D. Doll, J. Chem. Phys. **80**, 5832 (1984).